Journal of the Physical Society of Japan
Vol. 75, No. 4, April, 2006, 044602

Observation of Low-Temperature Elastic Softening due to Vacancy in Crystalline Silicon

Terutaka GOTO*, Hiroshi YAMADA-KANETA[1], Yasuhiro SAITO, Yuichi NEMOTO, Koji SATO, Koichi KAKIMOTO[2] and Shintaro NAKAMURA[3]

Graduate School of Science and Technology, Niigata University, Niigata 950-2181
[1]*Atsugi Laboratories, Fujitsu Ltd., Morinosato-Wakamiya, Atsugi, Kanagawa 243-0197*
[2]*Research Institute for Applied Mechanics, Kyushu University, Fukuoka 816-8580*
[3]*Center for Low Temperature Science, Tohoku University, Sendai 980-8577*

(Received December 9, 2005; accepted February 20, 2006; published April 10, 2006)

In challenging a direct observation of the vacancy in crystalline silicon, we have carried out low-temperature ultrasonic measurements down to 20 mK. The longitudinal elastic constants of non-doped and B-doped crystalline silicons, which were grown by a floating zone (FZ) method in commercial base, reveal the elastic softening proportional to the reciprocal temperature below 20 K. The applied magnetic fields turn the elastic softening of the B-doped FZ silicon to a temperature-independent behavior, while the fields up to 16 T do not affect the elastic softening of the non-doped FZ silicon. We present a plausible scenario for this result. Namely the vacancy with the non-magnetic charge state V^0 in the non-doped silicon and the magnetic V^+ in the B-doped silicon is responsible for the low-temperature softening of the shear elastic constants $(C_{11} - C_{12})/2$ and C_{44}, which can be described in terms of the quadrupole susceptibility due to the Jahn–Teller effect.

KEYWORDS: vacancy, elastic softening, quadrupole susceptibility, Jahn–Teller effect, ultrasound, crystalline silicon
DOI: 10.1143/JPSJ.75.044602

1. Introduction

The silicon crystal is known to be the most pure and ideal crystal that the human being is able to handle. However, the silicon crystal grown at its melting point of 1412 °C inevitably leads to a finite concentration of the native point defects of the vacancy and/or silicon interstitial. The free energy containing the entropy term at finite temperatures is minimized for the crystal in which the regular lattice sites and the native point defects coexist. The vacancy is a point defect simply defined as an empty lattice site in crystalline silicon. The silicon interstitial is a point defect of a silicon atom that resides at one of the interstices of the silicon lattice. The rate of the crystal growth in floating zone (FZ) and Czockralski (CZ) furnaces determins the native defect species: either the vacancy or interstitial.[1)] A fast growth-rate leads to vacancy-rich crystal, while a slow growth-rate favors interstitial-rich crystal.

The vacancy-rich wafer is generally adopted in device fabrications. The vacancies precipitate to form voids with octahedral shape being 100 nm in typical size. The existence of single vacancies is indirectly inferred from observations of the voids. The crystal-originated particle (COP) after $NH_4/H_2O_2/H_2O$ cleaning is available for observations of the voids on the surface of wafer.[2)] The voids in bulk of crystalline silicon are detected by infrared light scattering tomography.[3)] The voids residing on the wafer surface and beneath the surface reduce the production yield of devices. The modern silicon-based integrated circuit requires to adopt the pure crystal being free from the grown-in defects of the COP and the void. The pure crystal is carefully prepared from the vicinity of the oxidation-induced stacking fault ring (OSF-ring) in the CZ iongot.[4–6)] Since the invention of the semiconductor devices more than half century ago, the direct observation of the isolated single vacancy in crystalline silicon has not been achieved yet. The increasing adoption of the pure crystal in the point-defect-controlled CZ silicon for the wafers in modern semiconductor technology requires the development of the direct observation of the vacancy in the pure crystal.

The removal of silicon single atom to form the vacancy leads to the defect molecular orbitals, which arise from the four sp^3 orbitals of the radicals bordering vacancy.[7)] The defect molecular orbitals of the vacancy at the tetrahedral T_d symmetry site split into a node-less singlet ground state with $\Gamma_1(A_1)$ symmetry and an excited triplet state with $\Gamma_5(T_2)$ symmetry at about 1.7 eV.[8)] The electron paramagnetic resonance[9)] and positron lifetime measurements[10)] were made to elucidate the vacancies that are intentionally created by electron bombardments or γ-ray irradiations. Schlüter carried out theoretical studies based on the density functionals, taking into account the electron–electron correlation and the electron-lattice coupling of silicon atoms surrounding the vacancy.[11,12)]

There are multi-charge states depending on the number of the electrons residing at the vacancy. The positively charged state V^+ possessing three electrons is dominant in the B-doped silicon donating hole states. Two of the three electrons occupy the ground state Γ_1 with anti-parallel spin orientation. The third electron occupies one of the triply degenerate Γ_5 states, which couple to the elastic strains through the Jahn–Teller effect. The charge state V^+ with unpaired spin shows magnetism, which is observable by the electron paramagnetic resonance (EPR). Adding one more electron to the charge state V^+ leads to neutral vacancy V^0 being created in the non-doped silicon. In the neutral vacancy V^0, the electrons with anti-parallel spins occupy one of the triply degenerate Γ_5 states. The pair of the electrons

*E-mail: goto@phys.sc.niigata-u.ac.jp

with anti-parallel spins of the neutral vacancy V^0 should be completely silent for external magnetic fields. The negatively charged state V^- possessing five electrons in the silicon with donor impurities shows magnetism and thereby can be detected by the EPR experiments. The local lattice distortion around the charge states V^+ and V^- of vacancies, which were intentionally created by electron-beam and γ-ray irradiations, were observed by the EPR.[9] This distortion is caused by the cooperative Jahn–Teller effect among the highly irradiated vacancies being strongly coupled each other.[11,12] As is shown in the present paper, however, the charge state of the thermally created vacancies with the extremely low concentration in the FZ silicon crystal shows no sign of the local distortion.

The doping effects in the elastic constants of n-type germanium[13] and n-type silicon[14] were already reported in 1960's. The ultrasonic attenuations of microwave phonons with 10 GHz region in donor and accepter impurities in silicon[15,16] were also argued. These results, however, did not mention the vacancy contribution to the low-temperature elastic properties, which will be described in the present paper. The decreasing of the sound velocity $\Delta v/v \sim 10^{-6}$ below 0.1 K down to 4 mK of high-purity single crystal silicon was found by using the high-Q mechanical-oscillator technique.[17] Furthermore the elastic softening of the neutron irradiated silicon crystal below a few Kelvin was reported.[18] These low-temperature elastic softening, however, were described in terms of the two-level system, which is characteristic for the atomic tunneling excitation in "glassy" compounds.[19] The low-temperature elastic softening due to the charge states of the vacancy in crystalline silicon has not been reported so far.

2. Experimental

In the present paper, we show that the low-temperature ultrasonic measurements are usefull for the direct observation of the vacancy in crystalline silicon. We used two different silicon species in commercial base: non-doped FZ silicon and B-doped FZ silicon. The latter B-doped FZ silicon possesses resistivity 10 Ω cm at room temperature. These FZ crystals were grown in fast growth rate and are thereby expected to include thermally created vacancies with concentration of $N = N_0 \exp(-E_f/k_B T)$. Here, N_0 is the number of silicon atoms in unit volume and E_f is a vacancy formation-energy.

The piezoelectric ZnO film with 10 μm in thickness, whose hexagonal c-axis is orienting perpendicular to the surface of silicon crystals, was fabricated to generate and detect the longitudinal ultrasonic wave with frequencies of 400 MHz. A homemade ultrasonic apparatus based on the phase difference detection was used for the measurements of the ultrasonic velocity v in a high resolution of $\Delta v/v \sim 10^{-6}$. This high resolution was crucially important for the detection of small amount of elastic softening in the present experiments. The conventional $LiNbO_3$ transducers of resonant frequencies 80–40 MHz with 40 μm in thickness was not employed in the present experiments because of its relatively deficient resolution. The elastic constants of silicon crystals were estimated by $C = \rho v^2$ with the mass density $\rho = 2.33\ \mathrm{g\,cm^{-3}}$. For the low-temperature ultrasonic measurements, we used a ^{3}He-refrigerator down to 450 mK and a ^{3}He–^{4}He dilution refrigerator down to 20 mK. The magnetic fields up to 16 T were generated by a superconducting magnet.

In the present measurements, we used the longitudinal ultrasonic waves propagating along the high symmetry [001], [110], and [111] axes of crystalline silicon.[20] The elastic constant $C_{11} = C_B + (4/3)(C_{11} - C_{12})/2$ was measured by the longitudinal ultrasonic wave propagating along the [001] axis, which induces the elastic strain $\varepsilon_{zz} = (1/3)\varepsilon_B + (1/\sqrt{3})\varepsilon_u$. Here, the tetragonal strain $\varepsilon_u = (1/\sqrt{3})(2\varepsilon_{zz} - \varepsilon_{xx} - \varepsilon_{yy})$ with Γ_3 symmetry is responsible for the elastic constant $(C_{11} - C_{12})/2$ and the full symmetry volume strain $\varepsilon_B = \varepsilon_{xx} + \varepsilon_{yy} + \varepsilon_{zz}$ for the bulk modulus $C_B = (1/3)(C_{11} + 2C_{12})$. The elastic constant $C_{L[111]} = C_B + (4/3)C_{44}$ was obtained by the longitudinal wave along the [111] axis, which induces the elastic strain $\varepsilon_{L[111]} = (1/3)\varepsilon_B + (2/\sqrt{3})\varepsilon_{trigonal}$. The trigonal strain $\varepsilon_{trigonal} = (1/\sqrt{3})(\varepsilon_{yz} + \varepsilon_{zx} + \varepsilon_{xy})$ with Γ_5 symmetry is responsible for C_{44}. The longitudinal wave along the [110] direction of the elastic constant $C_{L[110]} = C_B + (1/3)(C_{11} - C_{12})/2 + C_{44}$ induces the strain of $\varepsilon_{L[110]} = (1/2)(\varepsilon_{xx} + \varepsilon_{yy}) + \varepsilon_{xy} = (1/3)\varepsilon_B - (1/2\sqrt{3})\varepsilon_u + \varepsilon_{xy}$.

3. Results

The elastic constant $C_{L[111]}$ of the non-doped FZ silicon in zero magnetic field, which is shown by open circles in Fig. 1, exhibits a softening of 0.8×10^{-4} below 20 K down to 20 mK. The softenings of $C_{L[111]}$ in applied magnetic field of 5 T shown by open triangles and of 10 T by open squares coincide with the zero-field softening. From the precise measurements of the softening in the longitudinal elastic constants for the high symmetry crystal axes, we conclude that the shear moduli of C_{44} and $(C_{11} - C_{12})/2$ reveal the elastic softening. Furthermore, the bulk modulus C_B is deduced to be of temperature-independence at low temperatures. The C_{44} in the right vertical scale of Fig. 1 was calculated from the experimental result of $C_{L[111]}$ in the

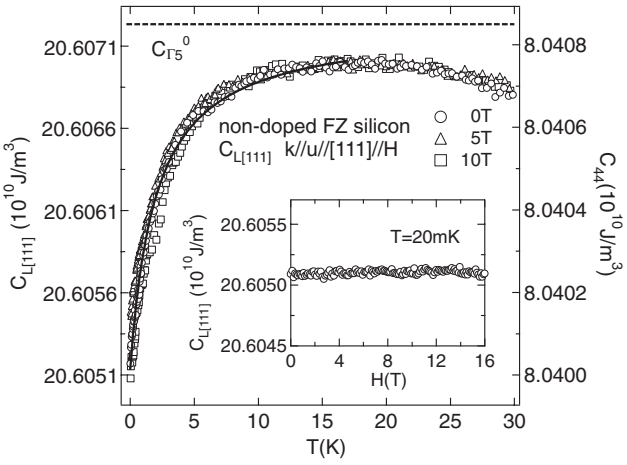

Fig. 1. Temperature dependence of $C_{L[111]}$ down to 20 mK in non-doped FZ silicon measured by the longitudinal ultrasonic wave propagating along the [111] axis. Open circles, triangles, and squares are the results under magnetic fields along the [111] axis of 0, 5, and 10 T, respectively. C_{44} of right hand scale was obtained by $C_{L[111]}$ by subtracting the temperature-independent C_B. The solid line is a fit with eq. (5) in the text. The inset shows the magnetic field dependence of $C_{L[111]}$ at base temperature 20 mK.

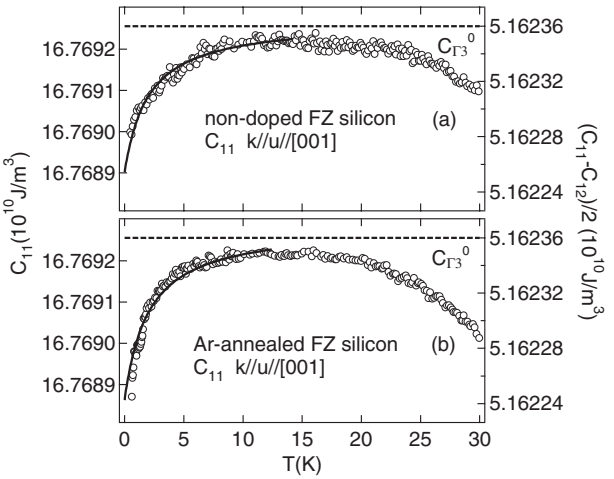

Fig. 2. Temperature dependence of C_{11} down to 450 mK in non-doped FZ silicon and Ar-annealed FZ silicon measured by the longitudinal ultrasonic wave propagating along the [001] axis. $(C_{11} - C_{12})/2$ of right hand scale was obtained by C_{11} by subtracting the temperature-independent C_B. The solid lines are fits with eq. (5) in the text.

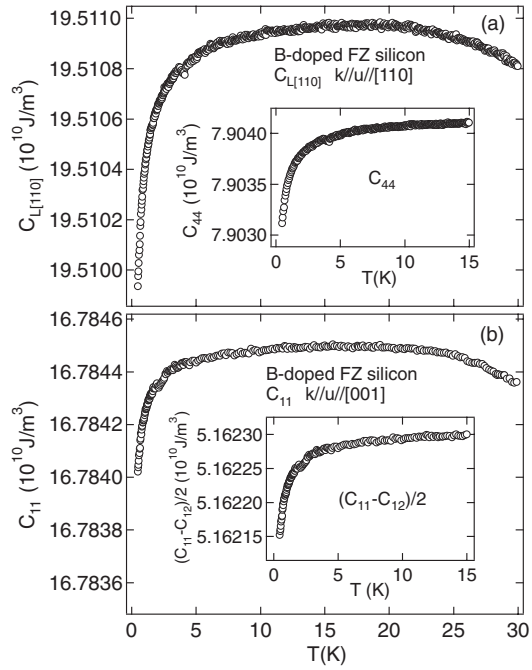

Fig. 3. Temperature dependence of $C_{L[110]}$ in (a) and C_{11} in (b) down to 450 mK of B-doped FZ silicon measured by the longitudinal ultrasonic wave propagating along the [110] and [001] axes, respectively. The inset shows the temperature dependence of C_{44} and $(C_{11} - C_{12})/2$ of B-doped FZ silicon obtained from $C_{L[110]}$ and C_{11} by subtracting the temperature-independent C_B.

left scale by subtracting the bulk modulus $C_B = 9.886 \times 10^{10}$ J/m^3. No dependence of the elastic constant $C_{L[111]}$ on the magnetic fields up to 16 T at base temperature 20 mK, which is presented in the inset of Fig. 1, confirms the non-magnetic character of the softening in the non-doped FZ silicon. The solid line in Fig. 1 is a fit, which will be discussed later.

As shown in Fig. 2(a), the elastic constant C_{11} of the non-doped FZ silicon exhibits a softening with decreasing temperature down to 450 mK. This behavior resembles in the softening of $C_{L[111]}$ of Fig. 1. The $(C_{11} - C_{12})/2$ in the right vertical scale of Fig. 2(a) is obtained from the softening of C_{11} by subtracting the temperature-independent bulk modulus C_B. The solid line in Fig. 2(a) is a fit that will be explained later. It is inferred that the low-temperature softening of $C_{L[111]}$ in Fig. 1 and of C_{11} in Fig. 2(a) originates from the native point defect of either the vacancy or the interstitial in crystalline silicon. Since the present non-doped FZ silicon crystal has high resistivity more than 10^3 Ω cm at room temperature, it is extremely pure and contains much less than 10^{13} cm^{-3} in impurity concentration.

In order to check whether the vacancies or silicon interstitials are responsible for the softening of C_{11} in the non-doped FZ silicon, we annealed the FZ silicon sample at 1350 °C for 10 h in ambient argon atmosphere. The concentration of the vacancy in the present condition is expected to be at least two orders of magnitude larger than that of silicon interstitials. The elastic constant C_{11} of the Ar-annealed FZ silicon in Fig. 2(b) exhibits a softening below 20 K similar to the softening in C_{11} of the non-doped FZ silicon in Fig. 2(a) before annealing. This result strongly suggests that the low-temperature softening of C_{11} in Fig. 2(a) is caused by the vacancy, the charge state V^0 possessing the non-magnetic character, in the non-doped FZ silicon.

The ultrasonic measurements of the B-doped FZ silicon may provide us with further information about the origin of the low-temperature elastic softening, because the charge state V^+ is expected in bulk. In zero magnetic field, the longitudinal elastic constant $C_{L[110]}$ of the B-doped FZ silicon in Fig. 3(a) and C_{11} in Fig. 3(b) show a softening with decreasing temperature below 20 K down to 450 mK. These softenings of $C_{L[110]}$ and C_{11} are consistently described by the softening of both $(C_{11} - C_{12})/2$ and C_{44} and a temperature-independent behavior of the bulk modulus C_B at low temperatures. The inset of Fig. 3(b) shows a softening of $(C_{11} - C_{12})/2$, which was calculated from C_{11} of Fig. 3(b) by subtracting the temperature-independent bulk modulus C_B. The softening of C_{44} in the inset of Fig. 3(a) is obtained from $C_{L[110]}$ of Fig. 3(a) by subtracting $(C_{11} - C_{12})/2$ in the inset of Fig. 3(b) and the temperature-independent bulk modulus C_B.

The magnetic field effect in the elastic softening of the B-doped FZ silicon is important to examine the charge state V^+ with magnetic character. As C_{11} of the B-doped FZ silicon shows in Fig. 4, the softening of $\Delta C_{11}/C_{11} = 3 \times 10^{-5}$ below 20 K down to 450 mK in zero field is appreciably reduced by applied magnetic field of 1 T. The applied field of 2 T suppresses the softening of C_{11}. The C_{11} in magnetic fields above 3.5 T up to 10 T turns to a slight increase with decreasing temperature below 4 K. The characteristic field dependence in C_{11} of the B-doped FZ silicon is also shown in the inset of Fig. 4. At the temperature of 700 mK, the elastic constant C_{11} increases rapidly with increasing magnetic fields up to 2 T and turns to a field-independent behavior. The field dependence in C_{11} is reduced at higher temperature of 1.6 K. The absence of field dependence was found at temperatures above 4.3 K. From these results, we conclude that the vacancy, which is the charge state V^+ possessing magnetism in the B-doped FZ silicon, leads to the softening of C_{11} and its sizable field dependence.

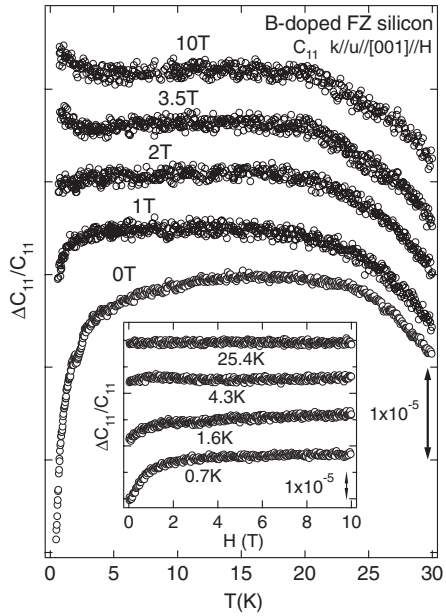

Fig. 4. The temperature dependence in $\Delta C_{11}/C_{11}$ of B-doped FZ silicon under applied magnetic fields along the [001] axis parallel to the propagation axis of the longitudinal ultrasonic wave. The inset shows the field dependence at temperatures of $T = 0.7$, 1.6, 4.3, and 25.4 K.

4. Analysis

The careful measurements of the longitudinal elastic constants along the high symmetry axes of the non-doped FZ and B-doped FZ silicon crystals indicate that shear moduli of $(C_{11} - C_{12})/2$ and C_{44} exhibit the softening below 20 K. The temperature independence of the bulk modulus $C_{\rm B}$ at low temperatures is deduced. In order to confirm the supposition that the bulk modulus is a constant at low temperatures, the accurate measurements of the transverse modes in addition to the longitudinal are required. In the present section, we analyze the low-temperature elastic softening of C_{44} and $(C_{11} - C_{12})/2$, which are obtained by the measurements of the longitudinal ultrasonic waves. For this purpose, the coupling of the charges states associated with vacancies to the elastic strain through the Jahn–Teller effect is introduced. Because of the overlapping integral due to the strong covalence bonding, the defect molecular orbitals consist of the fully symmetric singlet ϕ_{Γ_1} and the Γ_5 triplet $\phi_{\Gamma_{5x}}$, $\phi_{\Gamma_{5y}}$ and $\phi_{\Gamma_{5z}}$.[7] The direct product of the Γ_5 state is reduced to the direct sum of the irreducible representations as $\Gamma_5 \otimes \Gamma_5 = \Gamma_1 \oplus \Gamma_3 \oplus \Gamma_4 \oplus \Gamma_5$. This result means that the triply degenerate Γ_5 state associated with the charge state V^0 and V^+ possess the electric quadrupole moments Q_{Γ_γ} with the Γ_3 and Γ_5 symmetries, which couple to the elastic strains $\varepsilon_{\Gamma_\gamma}$ with the same symmetry.

The elastic softening of $C_{\Gamma_3} = (C_{11} - C_{12})/2$ and $C_{\Gamma_5} = C_{44}$ in particular is basically caused by the interaction of the electric quadrupoles of the charge state of the vacancy to the elastic strain as $H_{QS} = -\sum_{\Gamma_\gamma}\sum_i l_\Gamma Q_{\Gamma_\gamma}(i)\varepsilon_{\Gamma_\gamma}$.[21–23] Here, the $Q_{\Gamma_\gamma}(i)$ is the quadrupole moment of the defect orbitals of vacancy at site-i. For convinience, we introduce quadrupolar operators of $O_{\rm u} = (2\hat{z}^2 - \hat{x}^2 - \hat{y}^2)/\sqrt{3}$ and $O_v = \hat{x}^2 - \hat{y}^2$ of the Γ_3 symmetry and $O_{yz} = \hat{y}\hat{z}$, $O_{zx} = \hat{z}\hat{x}$ and $O_{xy} = \hat{x}\hat{y}$ of the Γ_5 symmetry, which act on the triply degenerate Γ_5 of charge state V^0 or V^+ at site i. Here, the coordinates $\hat{x} = x/r$, $\hat{y} = y/r$ and $\hat{z} = z/r$ with unit length for the electron at position $\boldsymbol{r} = (x, y, z)$ are used. In Table I, the multipoles and symmetry strains are listed together with the elastic constants C_Γ. The quadrupole moment for the charge state is evaluated as $Q_{\Gamma_\gamma} = q_\Gamma O_{\Gamma_\gamma}$ by using a coefficient $q_\Gamma = Z^* a^2$ for an effective charge Z^* and an effective radius a of the charge state. The quadrupole-strain interaction Hamiltonian is rewritten as

$$H_{QS} = -g_{\Gamma_3}\sum_i (O_{\rm u}(i)\varepsilon_{\rm u} + O_v(i)\varepsilon_v) - g_{\Gamma_5}\sum_i (O_{yz}(i)\varepsilon_{yz} + O_{zx}(i)\varepsilon_{zx} + O_{xy}(i)\varepsilon_{xy}). \quad (1)$$

Here, $g_\Gamma = l_\Gamma q_\Gamma = l_\Gamma Z^* a^2$ is a coupling constant. The perturbation due to a finite strain $\varepsilon_{\Gamma_\gamma}$ excited by the ultrasonic wave contributes to the electronic free energy as $F = -k_{\rm B}T \ln\{\sum_i \exp[-E_i(\varepsilon_{\Gamma_\gamma})/k_{\rm B}T]\}^N$. Here, $E_i(\varepsilon_{\Gamma_\gamma})$ is the energy for the Γ_5 state $\phi_{\Gamma_{5,i}}$ $(i = x, y, z)$ as a function of the elastic strain $\varepsilon_{\Gamma_\gamma}$ up to the second order and N is the number of the vacancy in unit volume. The quadrupole susceptibility χ_Γ is defined by the second derivative of the free energy with respect to the elastic strain $\varepsilon_{\Gamma_\gamma}$ as $(\partial^2 F/\partial\varepsilon^2_{\Gamma_\gamma})_{\varepsilon_{\Gamma_\gamma}\to 0} = -Ng^2_\Gamma\chi_\Gamma$.

The low-temperature softening of the elastic constant is affected by the long-range electric quadrupole interaction between the vacancies at different sites i and j, which is described as $H_{QQ} = -\sum_{\Gamma_\gamma}\sum_{i>j} l'_\Gamma Q_{\Gamma_\gamma}(i)Q_{\Gamma_\gamma}(j)$. Employing the quadrupole operators, one gets the inter-vacancy interactions as

Table I. The electric multipoles O_{Γ_γ} and corresponding symmetry strains $\varepsilon_{\Gamma_\gamma}$. They are needed to describe the coupling of the charge state in the vacancy to the elastic strain. The coordinates $\hat{x} = x/r$, $\hat{y} = y/r$ and $\hat{z} = z/r$ with unit length for the electron at position $\boldsymbol{r} = (x, y, z)$ are introduced. The elastic constants C_Γ responsible for the symmetry strains $\varepsilon_{\Gamma_\gamma}$ are also listed.

Symmetry	Multipole O_{Γ_γ}	Strain $\varepsilon_{\Gamma_\gamma}$	Elastic constant C_Γ
$\Gamma_1(A_1)$	$O_B = \hat{x}^2 + \hat{y}^2 + \hat{z}^2$	$\varepsilon_{\rm B} = \varepsilon_{xx} + \varepsilon_{yy} + \varepsilon_{zz}$	$\dfrac{C_{11} + 2C_{12}}{3}$
	$O_B^4 = \hat{x}^4 + \hat{y}^4 + \hat{z}^4 - \dfrac{3}{5}(\hat{x}^2 + \hat{y}^2 + \hat{z}^2)^2$		
$\Gamma_3(E)$	$O_{\rm u} = \dfrac{2\hat{z}^2 - \hat{x}^2 - \hat{y}^2}{\sqrt{3}}$	$\varepsilon_{\rm u} = \dfrac{2\varepsilon_{zz} - \varepsilon_{xx} - \varepsilon_{yy}}{\sqrt{3}}$	$\dfrac{C_{11} - C_{12}}{2}$
	$O_v = \hat{x}^2 - \hat{y}^2$	$\varepsilon_v = \varepsilon_{xx} - \varepsilon_{yy}$	
$\Gamma_5(T_2)$	$O_{yz} = \hat{y}\hat{z}$	ε_{yz}	C_{44}
	$O_{zx} = \hat{z}\hat{x}$	ε_{zx}	
	$O_{xy} = \hat{x}\hat{y}$	ε_{xy}	

$$H_{QQ} = -G'_{\Gamma_3}\sum_{i>j}(O_u(i)O_u(j) + O_v(i)O_v(j)) - G'_{\Gamma_5}\sum_{i>j}(O_{yz}(i)O_{yz}(j) + O_{zx}(i)O_{zx}(j) + O_{xy}(i)O_{xy}(j)). \quad (2)$$

Here, we use a coupling constant $G'_\Gamma = l'_\Gamma(q_\Gamma)^2 = l'_\Gamma(Z^*)^2a^4$. Using a mean field approximation of $H^{MF}_{QQ} = -\sum_{\Gamma_\gamma}\sum_i g'_\Gamma\langle O_{\Gamma_\gamma}\rangle O_{\Gamma_\gamma}(i)$, one gets the temperature dependence of the elastic constant described in terms of the quadrupole susceptibility χ_Γ as $C_\Gamma = C^0_\Gamma - Ng^2_\Gamma\chi_\Gamma/(1 - g'_\Gamma\chi_\Gamma)$. Here, the coupling constant $g'_\Gamma = zG'_\Gamma = zl'_\Gamma(Z^*)^2a^4$ is the inter-vacancy interaction for effective pair number z.

The longitudinal $C_{L[111]}$ mode induces the elastic strain $\varepsilon_{L[111]} = (1/3)\varepsilon_B + (2/\sqrt{3})\varepsilon_{trigonal}$. To estimate the perturbation energy through eq. (1) due to a finite strain of $\varepsilon_{yz} = \varepsilon_{zx} = \varepsilon_{xy} = \varepsilon/\sqrt{3} \neq 0$, it is necessary to calculate the matrix of the quadrupole operators for the triply degenerate Γ_5 states. Employing the Gell–Mann matrices for the SU(3) group with generators λ_i ($i = 1$–9), we obtain the quadrupole operators for the triply degenerate Γ_5 states as $O_{yz} = (1/\sqrt{2})(\lambda_5 - \lambda_7)$, $O_{zx} = (1/\sqrt{2})(\lambda_4 + \lambda_6)$ and $O_{xy} = -\lambda_2$:[24,25]

$$[O_{yz}] = \frac{1}{\sqrt{2}}\begin{bmatrix}0 & 0 & -i\\ 0 & 0 & i\\ i & -i & 0\end{bmatrix},\quad [O_{zx}] = \frac{1}{\sqrt{2}}\begin{bmatrix}0 & 0 & 1\\ 0 & 0 & 1\\ 1 & 1 & 0\end{bmatrix},$$
$$[O_{xy}] = \begin{bmatrix}0 & i & 0\\ -i & 0 & 0\\ 0 & 0 & 0\end{bmatrix}. \quad (3)$$

By using the matrices of eq. (3), one gets the quadrupole susceptibility $-g^2_{\Gamma_5}\chi_{\Gamma_5} = -(2/3)(g^2_{\Gamma_5}/k_BT) = -\delta^2_{\Gamma_5}/k_BT$ with the deformation energy $\delta_{\Gamma_5} = \sqrt{2/3}g_{\Gamma_5}$ for one vacancy. The $-g^2_{\Gamma_5}\chi_{\Gamma_5}$ describes the softening of the elastic constant $C_{\Gamma_5} = C_{44}$.

In the longitudinal C_{11} mode associated with the strain $\varepsilon_{zz} = (1/3)\varepsilon_B + (1/\sqrt{3})\varepsilon_u$, the strain $\varepsilon_u \neq 0$ with Γ_3 symmetry also gives a perturbation on the triply degenerate Γ_5 states of the vacancy. The matrices of the quadrupole operators of $O_u = \lambda_8$ and $O_v = \lambda_1$ are written as

$$[O_u] = \frac{1}{\sqrt{3}}\begin{bmatrix}1 & 0 & 0\\ 0 & 1 & 0\\ 0 & 0 & -2\end{bmatrix},\quad [O_v] = \begin{bmatrix}0 & 1 & 0\\ 1 & 0 & 0\\ 0 & 0 & 0\end{bmatrix}. \quad (4)$$

The quadrupole susceptibility $-g^2_{\Gamma_3}\chi_{\Gamma_3} = -(2/3)(g^2_{\Gamma_3}/k_BT) = -\delta^2_{\Gamma_3}/k_BT$ with the the deformation energy $\delta_{\Gamma_3} = \sqrt{2/3}g_{\Gamma_3}$ for one vacancy tells us the softening of $C_{\Gamma_3} = (C_{11} - C_{12})/2$. With decreasing temperature, the elastic constants $(C_{11} - C_{12})/2$ and C_{44} soften as

$$C_\Gamma = C^0_\Gamma\left(\frac{T - T_C}{T - \Theta}\right). \quad (5)$$

Here, we have introduced characteristic temperatures Θ and T_C. The former $\Theta = (2/3)g'_\Gamma$ means the inter-vacancy coupling energy. The latter $T_C = \Theta + \Delta_{JT}$ is the inter-vacancy coupling including the Jahn–Teller energy gain $\Delta_{JT} = N\delta^2_\Gamma/C^0_\Gamma$, which is mediated by the elastic strain ε_Γ. If we know the deformation-coupling energy δ_Γ, the experimental determination of the Jahn–Teller energy Δ_{JT} may lead to the vacancy concentration number as $N = \Delta_{JT}C^0_\Gamma/\delta^2_\Gamma$. Furthermore, we expect that the $\Theta = (2/3)zG'_\Gamma$ in eq. (5) also depends on the concentration number N through the effective pair number z and the inter-vacancy interaction G'_Γ in bulk.

The solid line of Fig. 1 for C_{44} in the non-doped FZ silicon is based on eq. (5). The fitting gives $T_C = -2.0019$ K, $\Theta = -2.0021$ K, $\Delta_{JT} = T_C - \Theta = 0.2$ mK and $C^0_{44} = C^0_{\Gamma_5} = 8.04085 \times 10^{10}$ J/m^3. The softening of $(C_{11} - C_{12})/2$ of the non-doped FZ silicon and Ar-annealed FZ silicon in Fig. 2(b) is fitted by the solid line with $T_C = -2.00205$ K, $\Theta = -2.00210$ K and $\Delta_{JT} = T_C - \Theta = 0.05$ mK and $C^0_{\Gamma_3} = 5.16236 \times 10^{10}$ J/m^3. The negative value of Θ for both C_{44} and $(C_{11} - C_{12})/2$ means the antiferro-type inter-vacancy interaction for the charge state V^0. Furthermore, the negative value of T_C indicates that the quadrupole fluctuation associated with the triply degenerate Γ_5 states of V^0 presents even at the base temperature of 20 mK. This result evidences the cubic site symmetry T_d at the vacancy site in the present non-doped FZ silicon. The local distortion due to the Jahn–Teller effect, which was actually observed in intentionally created vacancies of irradiated silicon crystals by the EPR measurements,[9] is irrelevant for the present non-doped FZ silicon with extremely low vacancy concentration. For analysis of the softening due to V^+ in the B-doped FZ silicon, further experiments in applied magnetic fields at lower temperatures down to 20 mK are required.

It is worthwhile to estimate the vacancy concentration in bulk by using the relation of $N = \Delta_{JT}C^0_\Gamma/\delta^2_\Gamma$ for C_{44} and $(C_{11} - C_{12})/2$, which exhibits the sizable amount of the low-temperature softenings. The experiments give the elastic constant $C^0_{\Gamma_5} = 8.04085 \times 10^{10}$ J/m^3 in Fig. 1 and the Jahn–Teller energy $\Delta_{JT} = T_C - \Theta = 0.2$ mK for the non-doped FZ. However, the deformation coupling energy δ_{Γ_5} is unknown at the present stage. Adopting the deformation energy $\delta_{\Gamma_5} \sim 3$ eV for the ε_{Γ_5} strain, one can deduce the vacancy concentration $N \sim 10^{15}$ cm^{-3} for the present non-doped FZ silicon. This vacancy concentration combined with $N = N_0\exp(-E_f/k_BT)$ for the melting point $T = 1685$ K and $N_0 = 5 \times 10^{22}$ cm^{-3} leads to the vacancy formation-energy $E_f \sim 2.5$ eV. If we employ the vacancy concentration $N \sim 10^{15}$ cm^{-3} and the results of $(C_{11} - C_{12})/2$ for the non-doped FZ silicon in Fig. 2(a) with $\Delta_{JT} = T_C - \Theta = 0.05$ mK and $C^0_{\Gamma_3} = 5.16236 \times 10^{10}$ J/m^3, the deformation energy $\delta_{\Gamma_3} \sim 1$ eV is obtained for the $(C_{11} - C_{12})/2$. It is smaller than $\delta_{\Gamma_5} \sim 3$ eV for the C_{44}.

The ultrasonic experiments on rare-earth compounds have shown that the localized 4f-electron orbit with the effective radius $a \sim 0.4$ Å[26] give the deformation energy $\delta_\Gamma \sim 0.02$ eV.[27] As was previously mentioned, the deformation energy δ_Γ of the triply degenerate Γ_5 states in the vacancy is proportional to square of the effective radius as $\delta_\Gamma = \sqrt{2/3}g_\Gamma = \sqrt{2/3}l_\Gamma Z^*a^2$. This simple relation may also be relevant for the 4f orbit in rare-earth systems. The triply degenerate Γ_5 orbits of the electron residing at the vacancy is extended over the second nearest neighbor with radius up to $a \sim 5$ Å,[12] because of the reduction of the Coulomb potential for the electrons embedded in medium with dielectric constant $\varepsilon = 11.7$. The radius $a \sim 5$ Å of the vacancy is one order of magnitude larger than $a \sim 0.4$ Å in the 4f orbit of rare-earth ion. The extended orbits of the Γ_5

orbital with radius $a \sim 5$ Å of the charge state in the vacancy lead to the enhanced deformation energy $\delta_\Gamma \sim 3$ eV, which is two order of magnitude larger than $\delta_\Gamma \sim 0.02$ eV of the 4f orbit in rare-earth compounds. We note that a similar relation of the deformation energy δ_Γ to the effective radius a has been found in other quantum systems: $\delta_\Gamma \sim 0.001$ eV for the off-center rattling and tunneling state of $La_3Pd_{20}Ge_6$ with $a \sim 0.1$ Å,[28] and $\delta_\Gamma \sim 0.5$ eV for the off-center tunneling state of OH^- impurity ion in NaCl with $a \sim 1.0$ Å.[29]

The Curie constant $K_\Gamma = \delta_\Gamma^2 = (2/3)g_\Gamma^2 = (2/3)l_\Gamma^2(Z^*)^2a^4$ in the quadrupole susceptibility $-g_\Gamma^2\chi_\Gamma = -K_\Gamma/k_BT$, which is proportional to the fourth power of the effective radius a, is largely enhanced of four order of magnitude in comparing to that in the 4f orbit in rare-earth compounds. Therefore, the gigantic Curie constant in the quadrupole susceptibility for one vacancy in the FZ silicon crystal is able to cause the sizable amount of the elastic softening. It is comparable to the softening caused by the ten thousand rare-earth ions in crystal. This is the reason why the present low-temperature ultrasonic measurements succeeded in direct observation of the vacancy with the extremely low-concentration in crystalline silicon. The strong electron-strain interaction of the vacancy orbital, which leads to the gigantic Curie constant of the quadrupole susceptibility, is a profitable character for the faithful method of the vacancy evaluation in the CZ silicon, which is crucially required in the modern technologies of the silicon wafer fabrication.

5. Conclusions

In the present paper, we have discovered a low-temperature softening of the elastic constants $(C_{11} - C_{12})/2$ and C_{44} in the non-doped and B-doped FZ silicon crystals in commercial base. The present finding indicates that the vacancy accompanying the triply degenerate states, the non-magnetic charge state V^0 in the non-doped silicon and the magnetic V^+ in the B-doped silicon, gives rise to the low temperature elastic softening through the Jahn–Teller effect. The gigantic Curie constant in the quadrupole susceptibility of the triply degenerate Γ_5 states of the charge state in the vacancy leads to the sizable amount of the softening in the FZ silicon with the extremely low-concentration of the vacancy. The direct observation of the isolated vacancy in the crystalline silicon using the low-temperature ultrasonic measurements may advance researches on the charge states of the vacancy in semiconductor physics and the vacancy control in semiconductor device technologies.

Acknowledgment

The present work was supported by Grant-in-Aid for the Creation of Innovations through Business-Academic-Public Sector Cooperation (No. 15404) of the Ministry of Education, Culture, Sports, Science and Technology of Japan. The authors thank Drs. M. Hourai, M. Sano, and T. Ono of SUMCO Corporation for stimulating discussions. We appreciate Professors K. Izumi and M. Nakao of Osaka Prefecture University for the annealing of FZ silicon crystal. The fabrication of the piezoelectric ZnO film was supported by Dr. Y. Furumura and Mrs. E. Haikata in Philtech Inc.

1) V. V. Voronkov: J. Cryst. Growth **59** (1982) 625.
2) J. Ryuta, E. Morita, T. Tanaka and Y. Shimanuki: Jpn. J. Appl. Phys. **29** (1990) L1947.
3) M. Kato, T. Yoshida, Y. Ikeda and Y. Kitagawa: Jpn. J. Appl. Phys. **35** (1996) 5597.
4) M. Hourai, H. Nishikawa, T. Tanaka, S. Umeno, E. Asayama, T. Nomachi and G. Kelly: in *Semiconductor Silicon 1998*, ed. H. R. Huff, U. Gosele and H. Tsuya (Electrochemical Society, Pennington, 1999) PV 98-1, p. 453.
5) H. S. Kim, K. S. Lee, B. Y. Lee, H. D. Yoo, S. H. Pyi. C. G. Koh, B. S. Hong and Y. W. Kim: Jpn. J. Appl. Phys. **40** (2001) L1286.
6) H. Tsuya: Jpn. J. Appl. Phys. **43** (2004) 4055.
7) C. A. Coulson and M. J. Kearsley: Proc. R. Soc. London, Ser. A **241** (1957) 433.
8) L. Lannoo, G. A. Baraff and M. Schlüter: Phys. Rev. B **24** (1981) 955.
9) G. D. Watkins and J. R. Troxell: Phys. Rev. Lett. **44** (1980) 593.
10) S. Dannefaer, P. Mascher and D. Kerr: Phys. Rev. Lett. **56** (1986) 2195.
11) G. A. Baraff, E. O. Kane and M. Schlüter: Phys. Rev. B **21** (1980) 5662.
12) M. Schlüter: *Proc. Int. School of Physics "Enrico Fermi"* (North-Holland, Amsterdam, 1985) p. 495.
13) L. G. Bruner and R. W. Keys: Phys. Rev. Lett. **7** (1961) 55.
14) J. J. Hall: Phys. Rev. **161** (1967) 756.
15) P. C. Kwok: Phys. Rev. **149** (1966) 666.
16) K. Suzuki and N. Mikoshiba: Phys. Rev. Lett. **28** (1972) 94.
17) R. N. Kleiman, G. Agnolet and D. J. Bishop: Phys. Rev. Lett. **59** (1987) 2079.
18) M. Coeck and C. Laermans: Phys. Rev. B **58** (1998) 6708.
19) W. A. Philips: Phys. Rev. Lett. **61** (1988) 2632.
20) C. Kittel: *Introduction to Solid State Physics* (John Wiley & Sons, 1996) Chap. 3.
21) M. Kataoka and J. Kanamori: J. Phys. Soc. Jpn. **32** (1972) 113.
22) P. Fulde, J. Keller and G. Zwicknagl: Solid State Phys. **41** (1988) 1.
23) P. Thalmeier and B. Lüthi: in *Handbook on the Physics and Chemistry of Rare Earths*, ed. K. A. Gschneider, Jr. and L. Eyring (North-Holland, 1991) Vol. 14, Chap. 96.
24) L. L. Schiff: *Quantum Mechanics* (McGraw-Hill/Kogakusha, 1968).
25) G. A. Gehring and K. A. Gehring: Rep. Prog. Phys. **38** (1975) 1.
26) Y. Ōnuki and A. Hasegawa: in *Handbook on the Physics and Chemistry of Rare Earths*, ed. K. A. Gschneider, Jr. and L. Eyring (North-Holland, 1995) Vol. 20, Chap. 135.
27) S. Nakamura, T. Goto, S. Kunii, K. Iwashita and A. Tamaki: J. Phys. Soc. Jpn. **63** (1994) 623.
28) T. Goto, Y. Nemoto, T. Yamaguchi, M. Akatsu, T. Yanagisawa, O. Suzuki and H. Kitazawa: Phys. Rev. B **70** (2004) 184126.
29) E. Kanda, T. Goto, H. Yamada, S. Suto, S. Tanaka, T. Fujita and T. Fujimura: J. Phys. Soc. Jpn. **54** (1985) 175.